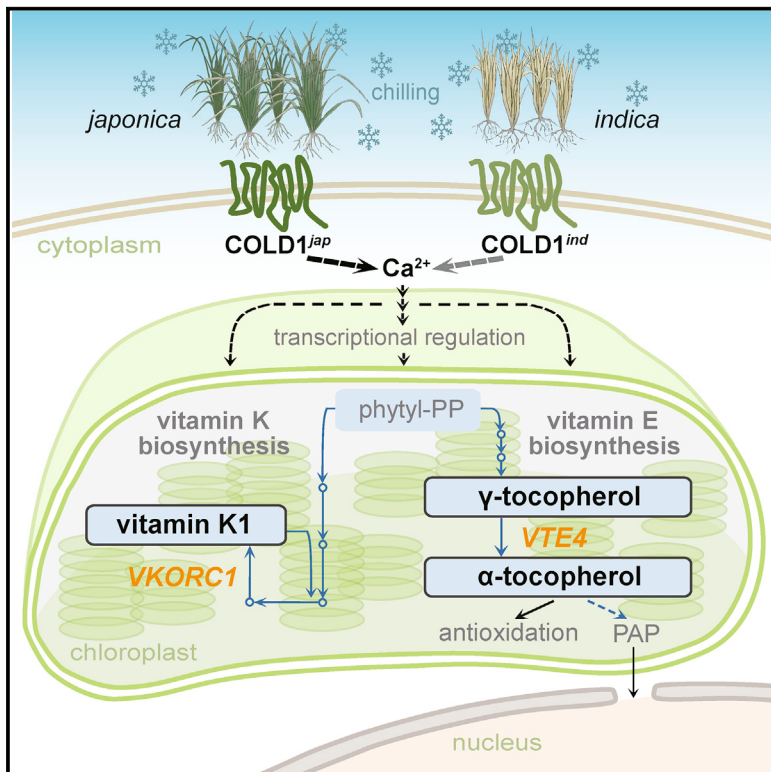


Integrated global analysis reveals a vitamin E-vitamin K1 sub-network, downstream of COLD1, underlying rice chilling tolerance divergence

Graphical abstract



Authors

Wei Luo, Qing Huan, Yunyuan Xu,
Wenfeng Qian, Kang Chong,
Jingyu Zhang

Correspondence

chongk@ibcas.ac.cn (K.C.),
jingyuzhang@ibcas.ac.cn (J.Z.)

In brief

Asian cultivated rice, *japonica* and *indica*, exhibit clearly different chilling tolerance. The underlying regulatory network, however, remains obscure. Luo et al. reveal a vitamin E-vitamin K1 sub-network in chloroplasts, downstream of cold sensor COLD1 and responsible for chilling tolerance divergence. The results suggest ways to improve stress tolerance in crops.

Highlights

- Vitamin E-vitamin K1 sub-network underlies rice chilling tolerance divergence
- The chloroplast is a regulation point in rice for different chilling tolerance
- Chilling signal transduced from membrane protein to chloroplast and then to nucleus



Article

Integrated global analysis reveals a vitamin E-vitamin K1 sub-network, downstream of COLD1, underlying rice chilling tolerance divergence

Wei Luo,^{1,4} Qing Huan,^{2,4} Yunyuan Xu,¹ Wenfeng Qian,^{2,3} Kang Chong,^{1,3,*} and Jingyu Zhang^{1,5,*}

¹Key Laboratory of Plant Molecular Physiology, Institute of Botany, Chinese Academy of Sciences, Beijing 100093, China

²State Key Laboratory of Plant Genomics, Institute of Genetics and Developmental Biology, Innovation Academy for Seed Design, Chinese Academy of Sciences, Beijing 100101, China

³University of Chinese Academy of Sciences, Beijing 100049, China

⁴These authors contributed equally

⁵Lead contact

*Correspondence: chongk@ibcas.ac.cn (K.C.), jingyuzhang@ibcas.ac.cn (J.Z.)

<https://doi.org/10.1016/j.celrep.2021.109397>

SUMMARY

Rice, a staple food with tropical/subtropical origination, is susceptible to cold stress, one of the major constraints on its yield and distribution. Asian cultivated rice consists of two subspecies with diverged chilling tolerance to adapt to different environments. The mechanism underlying this divergence remains obscure with a few known factors, including membrane protein CHILLING-TOLERANCE DIVERGENCE 1 (COLD1). Here, we reveal a vitamin E-vitamin K1 sub-network responsible for chilling tolerance divergence through global analyses. Rice genome regions responsible for tolerance divergence are identified with chromosome segment substitution lines (CSSLs). Comparative transcriptomic and metabolomic analysis of chilling-tolerant CSSL4-1 and parent lines uncovered a vitamin E-vitamin K1 sub-network in chloroplast with tocopherol (vitamin E) mediating chloroplast-to-nucleus signaling. COLD1, located in the substitution segment in CSSL4-1, is confirmed as its upstream regulator by transgenic material analysis. Our work uncovers a pathway downstream of COLD1, through which rice modulates chilling tolerance for thermal adaptation, with potential utility in crop improvement.

INTRODUCTION

Environmental temperature, one of the most important factors affecting plant growth and development, restricts crop productivity and distribution, especially for species that originated from tropical and subtropical regions, such as rice. As the staple food for more than one-half of the global population, rice is planted across a wide latitudinal range, including tropical and temperate zones. Asian cultivated rice has two major subgroups, namely, *japonica* and *indica*. Typical *japonica* rice, namely temperate *japonica*, exhibit more robust cold tolerance than *indica* and are mainly grown in areas with low environmental temperature. A major global cooling event that occurred approximately 4,200 years ago is the driving force for the diversification of temperate and tropical *japonica* (Gutaker et al., 2020). Temperature is likely the critical environmental factor driving rice evolution.

Cold stresses on plants are divided into different levels. Chilling (0–18°C) is typically experienced by plants from tropical or subtropical regions. In rice, chilling sensing and signaling pathways have been identified, with membrane protein CHILLING-TOLERANCE DIVERGENCE 1 (COLD1) as the sensor for cold signal (Ma et al., 2015; Körner, 2016). Chilling signal is first

perceived by G-protein regulator COLD1, which triggers calcium influx together with G-protein α subunit 1 (RGA1) and leads to activation of cold-responsive genes and other possible regulons (Ma et al., 2015; Moon et al., 2019). Other protein-kinase-mediated cold signaling pathways were also uncovered (Zhang et al., 2017, 2019). Chilling activates mitogen-activated protein kinase 3 (MPK3), which leads to the activation of trehalose-6-phosphate phosphatase 1 (*TPP1*) and the accumulation of trehalose. Rice chilling tolerance, therefore, increased with the aid of osmotic regulation (Zhang et al., 2017).

Japonica rice varieties, usually grown in higher latitude or altitude areas, exhibit more robust chilling tolerance than *indica* varieties grown in tropical and subtropical regions. Elucidating its underlying mechanism is critical for rice chilling tolerance improvement. A number of natural variations between *japonica* and *indica*, such as single nucleotide polymorphisms (SNPs), have been proven to contribute to their different chilling tolerance. COLD1 has a nonsynonymous SNP in the fourth exon, leading to different levels of RGA1 activation and cold-stimulated inward current signal and resulting in different chilling tolerance between *japonica* and *indica* (Ma et al., 2015; Manishankar and Kudla, 2015). One functional polymorphism in the exon of transcription factor *bZIP73* also contributes to cold tolerance



divergence (Liu et al., 2018). The nucleotide variations in the promoter region of *Ghd8* and *HAN1*, encoding a transcription factor and an oxidase finely regulating jasmonate (JA) -mediated chilling response, respectively, also lead to different chilling tolerance between *japonica* and *indica* (Mao et al., 2019; Wang et al., 2019a).

Chilling tolerance is a complex agricultural trait controlled by multiple genes (Guo et al., 2018). The diverged *japonica-indica* chilling tolerance, therefore, is unlikely to be attributed to one or two genes. It is of great importance to detect the regulatory pathway or network through a global analysis of the whole cold response system. In this study, we screened the rice genome with chromosome segment substitution lines (CSSLs), in which the genome of *indica* variety 93-11 was substituted segment by segment with *japonica* genomic DNA fragments, to identify the critical genomic region responsible for cold tolerance divergence (Xu et al., 2010). We obtained a substitution line CSSL4-1, whose chilling tolerance can be shifted to near the *japonica* level through the substitution of genomic segments. CSSL4-1, with *indica* background and near-*japonica* level chilling tolerance, is an ideal plant material to clarify the cold tolerance divergence mechanism. Thus, it was exposed to global transcriptional and metabolic profiling. Comparing CSSL4-1 and its parent lines helps to uncover response pathways mediated by the introgression genomic segment and reveal the regulation point by which plants modulate their chilling response system to adapt to different environments, paving the way for cold-tolerance molecular breeding.

RESULTS

The introgression of the NIP segment in 93-11 background results in CSSL4-1 with chilling tolerance similar to NIP

The chilling tolerance of *japonica* variety Nipponbare (NIP) and *indica* variety 93-11 was analyzed with different levels of chilling treatment. No phenotypic changes were observed after mild chilling treatment (4°C for 10 h) and recovery (normal temperature for 3 days) for both varieties. After severe chilling treatment (4°C for 41 h) and recovery, leaves of 93-11 severely wilted, but NIP still exhibited no noticeable phenotypic changes (Figures 1A and 1B), indicating that NIP and 93-11 have different cold tolerances.

To clarify the genetic basis for rice chilling tolerance divergence, we performed a screen with 62 CSSLs, in which various NIP chromosome segments were inserted into the 93-11 background (Xu et al., 2010). Twenty-two CSSLs showed cold tolerance higher than 93-11 (Figure S1A), among which CSSL4-1 was the most tolerant one. After severe chilling treatment and recovery, all NIP seedlings survived (survival rate, 100%) and only 4% of CSSL4-1 died (survival rate, 96%). The survival rate of 93-11 and other CSSLs, however, was lower (2%–59%; Figures 1A, 1B, S1A, and S1B). These findings suggest that the NIP segments inserted into CSSL4-1 can enhance the chilling tolerance of 93-11 to a level similar to that of NIP.

To study the molecular regulation mechanism contained in the NIP genomic segments in CSSL4-1, we searched this region for known chilling-tolerance-related quantitative trait loci (QTL). A QTL identified with recombinant inbred lines generated from a cross between *japonica* variety NIP and *indica* variety 93-11

was mapped to this region, with *COLD1* being the responsible gene (Ma et al., 2015; Figure S1C). To gain a comprehensive understanding of mechanisms underlying differential chilling tolerance between *japonica* and *indica*, we chose to use CSSL4-1, an ideal plant material with 93-11 background and near-NIP-level chilling tolerance, for further study.

Comparative transcriptomic analysis detects pathways showing similar change patterns for CSSL4-1 and NIP in chilling response

To identify transcriptional regulatory networks underlying the differential chilling tolerance between *japonica* and *indica*, high-throughput sequencing-based transcriptomic analyses were performed for CSSL4-1, NIP, and 93-11 with mild and severe chilling treatments (Figure 1C). For each sample, more than 40 million high-quality sequencing reads were obtained, and the expressions of more than 25 thousand genes were detected (Table S1). A significant proportion of them showed varied expression upon chilling treatment (Figures 2A and S2A). Quantitative real-time PCR was performed for verification (Figures S2B and S2C).

We performed a principal-component analysis (PCA) by using the expression levels of all detected genes, after being normalized by the expression levels in seedlings collected at the same growth stage without chilling treatment. Under mild chilling treatment, CSSL4-1 separated from both NIP and 93-11, probably reflecting the genetic incompatibility between NIP and 93-11. Under severe chilling treatment, CSSL4-1 clustered with 93-11, echoing that they shared the majority of their genetic background (Figure 2B).

To explore the mechanism responsible for *japonica-indica* divergence in cold tolerance, we attempted to identify genes that showed similar change patterns between CSSL4-1 and chilling-tolerant *japonica* variety NIP, but not chilling-sensitive *indica* variety 93-11 (see STAR Methods for details). These genes were further classified into the following four groups according to chilling treatment (10 h and 41 h) and change trend: 10 h up, 10 h down, 41 h up, and 41 h down. Then, we identified enriched pathways for different group of genes based on the Kyoto Encyclopedia of Genes and Genomes (KEGG) database using KEGG Orthology Based Annotation System (KOBAS) 3.0 (Xie et al., 2011). Multiple enriched ($p < 0.05$) pathways were identified and classified into different classes and subclasses according to their biological function. Two subclasses, namely, cofactors/vitamins and translation, contained obviously more pathways than others. Interestingly, in the cofactors/vitamin subclass the ubiquinone/terpenoid-quinone biosynthesis pathway and its related one, the diterpenoid biosynthesis pathway, were both identified (Figure 2C). Terpenoid and quinone biosynthesis includes the synthetic pathway of vitamin E (tocopherol) attaching to the photosynthetic membrane and vitamin K1 (phylloquinone), belonging to electron carriers in photosynthesis (Basset et al., 2017; Muñoz and Munné-Bosch, 2019).

Metabolic comparison reveals metabolites showing similar change patterns between CSSL4-1 and NIP in chilling response

We performed unbiased global metabolic profiling for CSSL4-1, NIP, and 93-11, in parallel with transcriptomic analyses

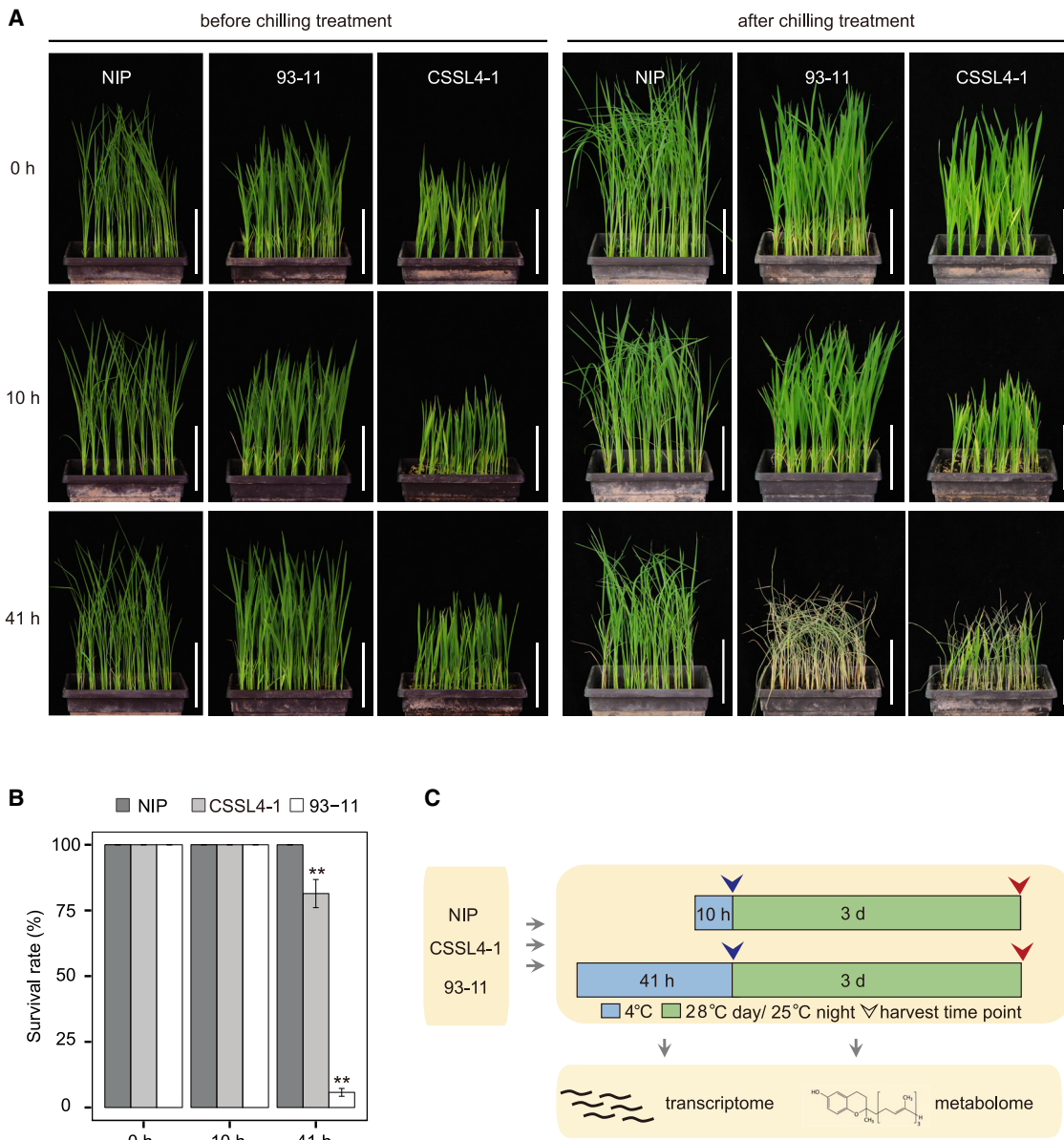


Figure 1. Chilling tolerance analysis of chromosome segment substitution line CSSL4-1 and experiment design

(A and B) Representative images and survival rates of substitution line CSSL4-1 and its parent lines NIP and 93-11 exposed to chilling treatment (4°C) for 10 and 41 h (10 h, 41 h) with recovery growth. Bar, 5 cm. Mean and standard deviation were calculated by at least three independent experiments. p values are given by the Student's t test with untreated plants as control (**p < 0.01).

(C) A schematic diagram shows the workflow. Parallel transcriptomic and metabolomic profiling were performed for substitution line CSSL4-1 and its parent lines NIP and 93-11 exposed to chilling treatment (4°C) 10 h and 41 h (10 h, 41 h), followed by 3 days (3 d) of recovery growth at a normal temperature (28°C day/25°C night). Blue and red arrows denote sampling time points of transcriptomic and metabolomic profiling, respectively.

(Figure 1C). A total of 305 metabolites were identified, and the average level of each metabolite in each sample was calculated from biological replicates. To eliminate the growth effect, metabolomic data from chilling-treated samples were normalized using those from corresponding untreated controls (Tables S2 and S3). The PCA plot of metabolomic data was different from that of the transcriptome. Under mild chilling treatment, CSSL4-1, NIP, and 93-11 clustered together. Under severe chilling treatment, how-

ever, CSSL4-1, 93-11, and NIP separated clearly on the PCA plot. CSSL4-1 and 93-11, with their similar background, grouped together to some extent, which is consistent with the results at the transcriptional level (Figures 2B and 3A). Interestingly, when PCA was performed just for samples of mild chilling treatment, the results showed that CSSL4-1, NIP, and 93-11 separated from one another with or without chilling treatment, suggesting that differences among these samples also exist

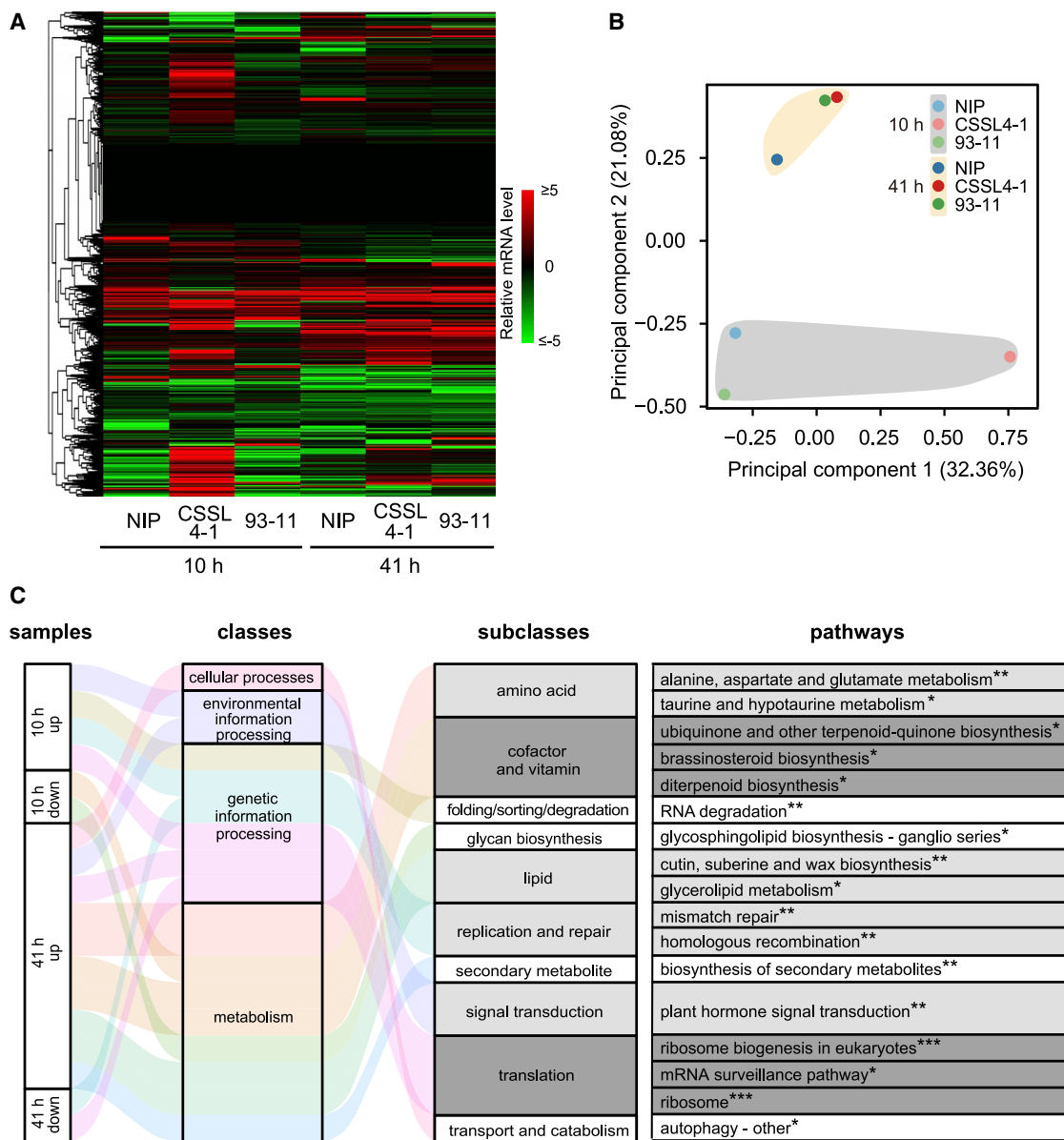


Figure 2. Transcriptomic comparison of CSSL4-1 and its parent lines, NIP and 93-11, under chilling stress

(A) Heatmap showing the effect of chilling stress on gene expression in CSSL4-1, NIP, and 93-11 with mild (10 h) and severe (41 h) chilling treatment. The mRNA expression changes in each sample were normalized by that in corresponding untreated samples and shown by different colors.

(B) Principal-component analysis for transcriptomic profiles of CSSL4-1, NIP, and 93-11 with mild and severe chilling treatment. The first two principal components explain 32.36% and 21.08% of the variance, respectively.

(C) Enrichment of pathways was performed based on Kyoto Encyclopedia of Genes and Genomes (KEGG) with KOBAS (KEGG Orthology Based Annotation System) 3.0 for genes showing similar change patterns between CSSL4-1 and NIP, but not 93-11, under chilling stress. Significantly enriched biological pathways are shown (* $p < 0.05$, ** $p < 0.01$, *** $p < 0.001$; hypergeometric test). Subclass sections are colored in gray (>2) or dark gray (>3) according to their containing biological pathway number. Connecting ribbons are colored according to the type of subclasses.

but are relatively weaker than those under severe chilling treatment, and may be covered up by the latter when they were analyzed together (Figures 3A, S3A, and S3B).

The content of various types of metabolites changed upon chilling stress, suggesting a profound effect of chilling stress on rice metabolism (Figure 3B). We detected the accumulation of a wide range of the amino acids and peptides under

severe chilling treatment, implying the disorder of their metabolism. The accumulation of peptides was relatively weak in NIP, echoing its high survival rate (Figures 1A, 1B, and 3B). The contents of lipids and carbohydrates increased for all three rice varieties upon severe treatment, implying lipid metabolism is a general response to chilling temperature (Figure 3B).

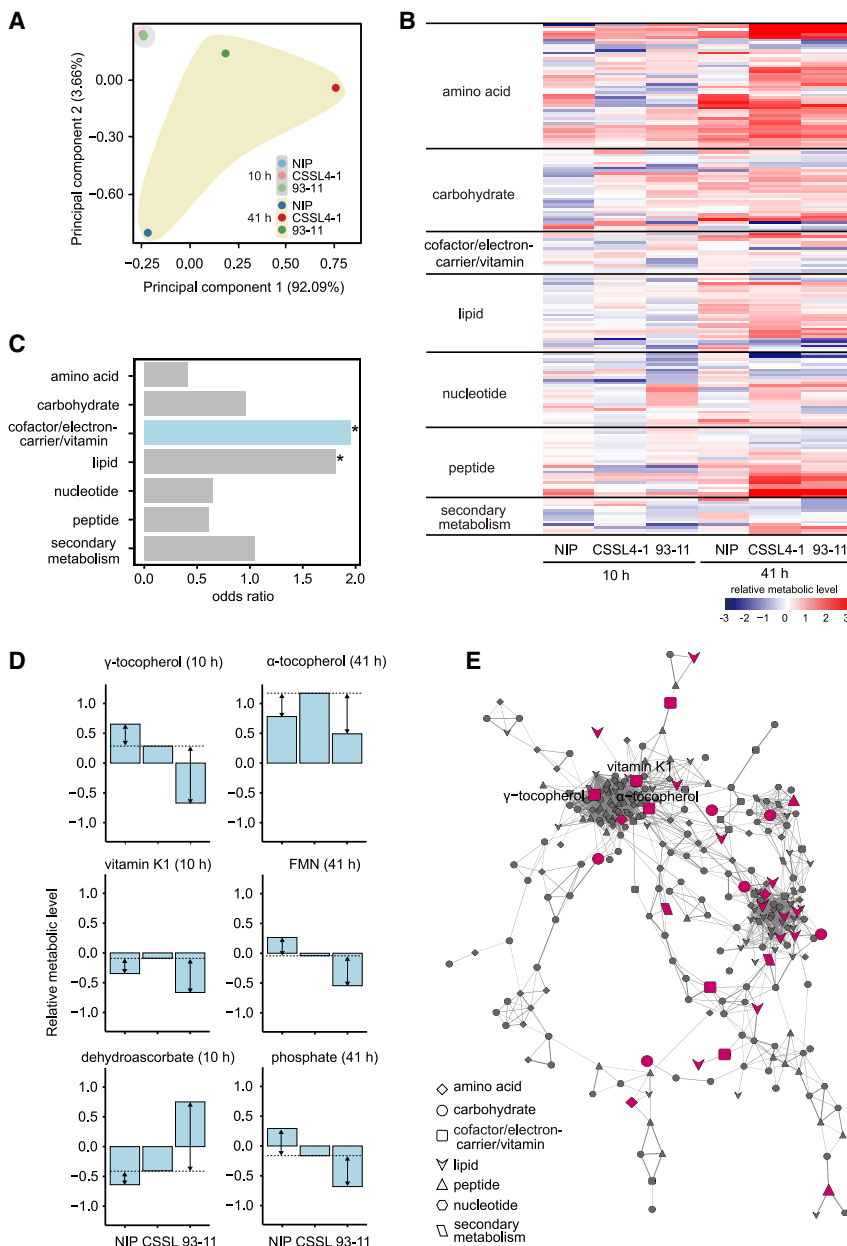


Figure 3. Metabolomic comparison of the response of CSSL4-1 and its parent lines, NIP and 93-11, under chilling stress

(A) Principal-component analysis of metabolic profiles of CSSL4-1, NIP, and 93-11 with mild and severe chilling treatment. The first two principal components explain 92.09% and 3.66% of the variance, respectively.

(B) Heatmap of chilling-induced changes in the content of detected metabolites in CSSL4-1, NIP, and 93-11 under mild (10 h) and severe (41 h) chilling treatment. Metabolic changes in each sample were normalized by that in the corresponding untreated samples and shown by different colors.

(C) The enrichment for different categories of chilling-tolerance-divergence-related metabolites, shown as odds ratio with the whole metabolome as background. Blue color denotes the most apparent enrichment. * $p < 0.05$, hypergeometric test. Details are shown in Figures 3D and S3C and Table S6.

(D) Relative changes of chilling-tolerance-divergence-related metabolites in the cofactor/electron carrier/vitamin category (Figure 3C), in CSSL4-1 (CSSL), NIP, and 93-11 under mild (10 h, left column) or severe (41 h, right column) chilling treatment. The relative metabolic level for each sample was normalized by that in the corresponding untreated samples, with \log_2 transformation. Dashed lines denote the level of CSSL4-1, and arrows denote the difference between CSSL4-1 and NIP or CSSL4-1 and 93-11.

(E) Weighted co-expression network of metabolites with mild and severe chilling treatment, based on Pearson's correlation coefficient with a threshold of 0.1. Chilling-tolerance-divergence-related metabolites are enlarged and colored in purplish red. The names of vitamin E (α -tocopherol) and vitamin K1 are labeled. Details are shown in Figure S4A.

Antioxidative response and related metabolic adjustment were also detected. The accumulation of putrescine, a polyamine possessing antioxidant activities, was observed initially in NIP and then in CSSL4-1 and 93-11 as the treatment level increased (Cuevas et al., 2008; Verma and Mishra, 2005). It is also the same case for glutamine and glutamate, metabolites related to the glutathione-ascorbate cycle (Table S4; Noctor et al., 2012; Ohkama-Ohtsu et al., 2008). Upon mild treatment, an increase was detected in NIP for nicotinamide ribonucleotide (NMN), an intermediate in nicotinamide adenine dinucleotide (NAD) synthesis, which is involved in plant cellular redox homeostasis (Hashida et al., 2009; Jayaram et al., 2011). The increase was detected both in NIP and CSSL4-1 under severe treatment,

but never observed for 93-11, consistent with the relatively higher chilling tolerance for CSSL4-1 and NIP (Figures 1A and 1B; Table S4).

To identify the functional metabolites contributing to the higher chilling tolerance of CSSL4-1 and NIP, we chose metabolites showing similar changes between CSSL4-1 and *japonica* variety NIP but different between CSSL4-1 and *indica* variety 93-11 (see STAR Methods for details). A total of 39 candidate metabolites, eligible under either mild (10 h) or severe (41 h) chilling treatment, were selected as chilling-tolerance-divergence-related metabolites, including amino acids and peptides, carbohydrates, lipids, nucleotides, cofactors, vitamins, and secondary metabolites (Table S5). The most apparent enrichment ($p < 0.05$, hypergeometric test) was observed for cofactors/electron carriers/vitamins, including vitamin E (tocopherol) and vitamin K1, echoing the transcriptional analysis results (Figures 2C, 3C, and 3D; Table S6).

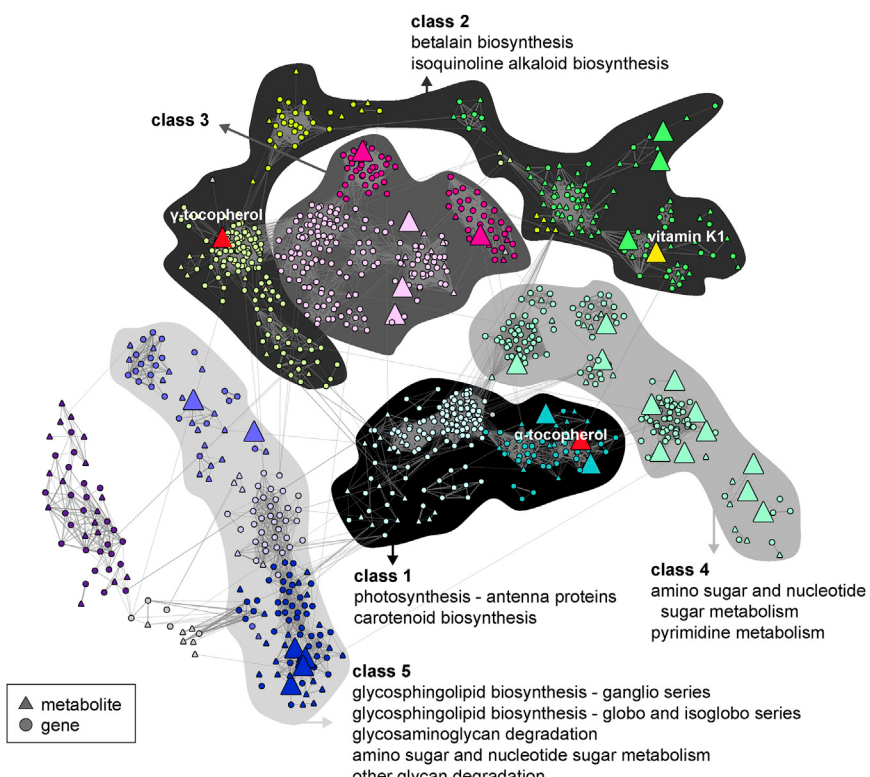


Figure 4. Network showing connection between transcriptome and metabolome in chilling stress response

Weighted co-expression network of highly variable (their variance ranked at the top 5%) genes and metabolites with mild and severe chilling treatment, based on Pearson's correlation coefficient with a threshold of 0.2. Classes 1–5 are outlined with different colors. The name of pathways under classes 1–5 resulted from KEGG pathway enrichment analysis ($p < 0.05$, hypergeometric test, only top 5 were shown) (Table S9). Chilling-tolerance-divergence-related metabolites are denoted with big triangles, filled with colors of corresponding modules. The triangles for vitamin E (α -tocopherol and γ -tocopherol) and vitamin K1 are highlighted with red and yellow color, respectively. Details are shown in Figures S4B–S4D and Tables S8 and S9.

Both vitamin E and vitamin K1 are mainly synthesized in the chloroplast, and their biosynthesis is part of the ubiquinone/terpenoid-quinone biosynthetic network and has a common precursor, phytol-PP (PDP). The biosynthetic pathways of vitamin E and vitamin K1 form a sub-network (Basset et al., 2017; Mène-Saffrané, 2017). We also analyzed nucleotide diversity of this sub-network. Only one gene, namely, *VTE4* encoding tocopherol O-methyltransferase, was found to possess two nonsynonymous SNPs that are different between *japonica* and *indica*, implying that it is the one exposed to divergence-related natural selection (Table S7; Bergmüller et al., 2003). Enrichment ($p < 0.05$, hypergeometric test) was also detected for phospholipids in membrane, phosphoethanolamine, oleoylglycerophosphocholine, and linoleylglycerophosphocholine (Figures 3C and S3C; Table S6), which might be the polyunsaturated membrane lipids protected by tocopherol against peroxidation (Chen et al., 2009; Hullin-Matsuda et al., 2016; Sánchez-Migallón et al., 1996). The 12,13-hydroxyoctadec-9(Z)-enoate, whose metabolism is associated with waxes, was also detected, in concert with the appearance of wax biosynthesis in enriched pathway analysis of genes with similar change patterns between CSSL4-1 and NIP at the transcriptional level (Figures 2C and S3C; Kosma et al., 2015).

We constructed a co-variation network from the metabolic profiles to explore the relationship among metabolites. The network, containing 296 nodes (metabolites) and 2,145 edges (co-variation relationship), included 2 core modules (Figures 3E and S4A). Vitamin E and its biosynthesis-related metabolites

are mainly located in the larger core module, suggesting synchronized regulation in chilling response. Vitamin K1 also locates in the same core module, consistent with the fact that vitamins E and K form a sub-network. Approximately one-third of the 39 diverged-chilling-tolerance-related compounds were also located in the core areas, suggesting

the adaptation of the vital regulatory point underlying chilling tolerance divergence (Figure 3E).

Integrative analyses of metabolomics and transcriptomics reveal a critical role of the vitamin E-vitamin K1 sub-network

We constructed weighted co-expression networks from the profiles comprising metabolite levels together with transcriptional data from CSSL4-1, NIP, and 93-11 with mild and severe chilling treatment. The edges in such networks were established between two nodes if the corresponding variables were significantly correlated based on Pearson's correlation coefficient. This network included 830 highly variable genes (ranked at the top 5%) and 259 metabolites. A total of 12,468 edges and 12 modules were identified, which were further grouped into 5 classes (Figures 4 and S4B–S4D; Table S8). Class 1, with genes largely related to photosynthesis, contained the largest number of connections, implying a significant association between transcriptional and metabolic levels for this biological process (Tables S8 and S9).

To uncover the role of diverged-chilling-tolerance-related compounds in the whole regulation system, their position in the co-expression network was analyzed. α -Tocopherol is located in class 1, consistent with its function in photosynthetic antioxidation. γ -Tocopherol and vitamin K1 are located in class 2, consistent with their chemical structures. Interestingly, α -tocopherol and γ -tocopherol belong to two different classes, suggesting a difference in function and interaction with other metabolites. Classes 1–4 are close to each other and compose a relatively

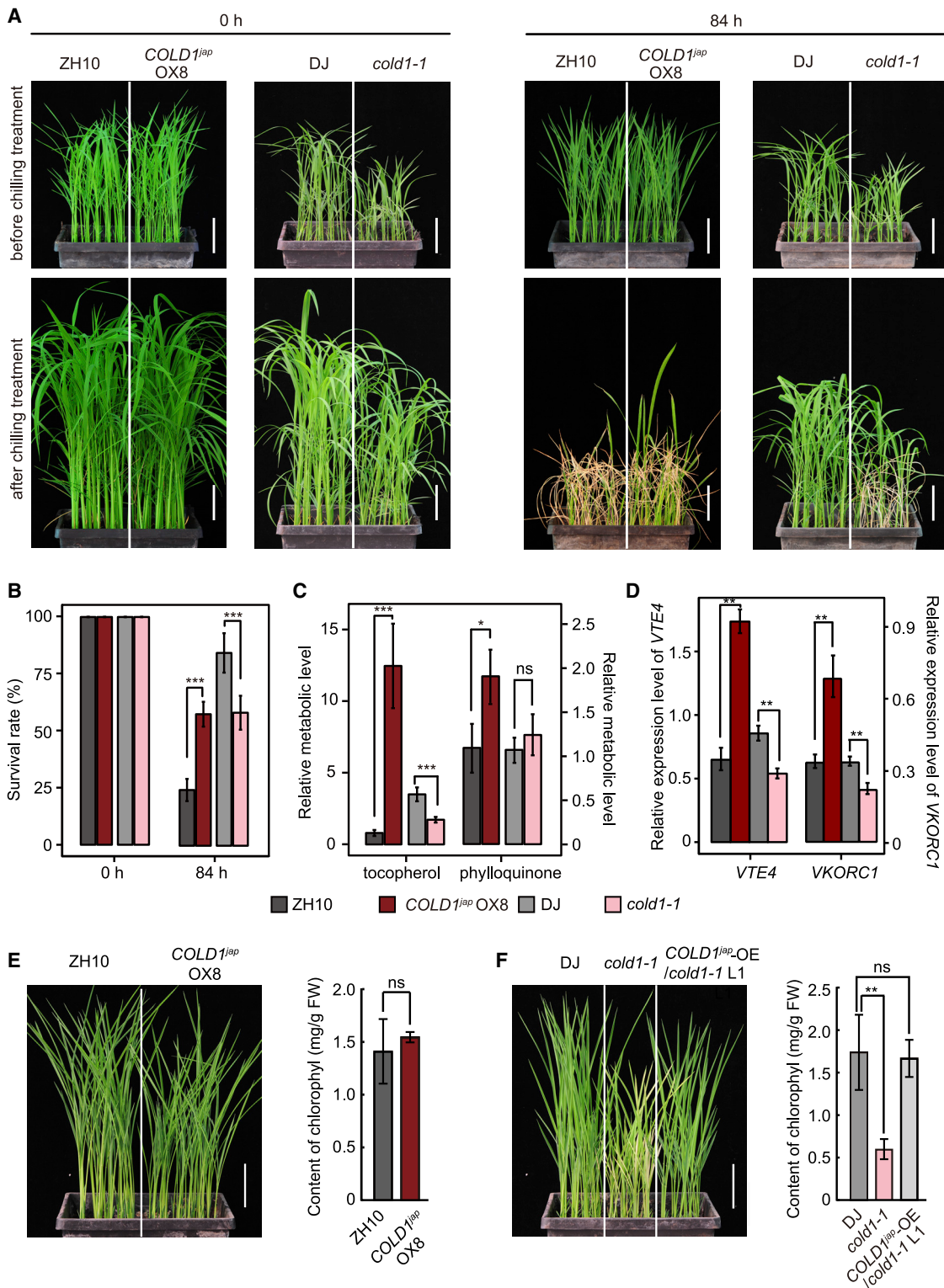


Figure 5. Analysis of transgenic materials for *COLD1*

(A) Representative images of *COLD1* overexpression line (*COLD1^{lap}OX8*) and mutant (*cold1-1*) after chilling treatment for 0 and 84 h with recovery growth, with Zhonghua 10 (ZH10) and Dongjin (DJ) as corresponding controls. Bar, 5 cm.
 (B) Survival rate of *COLD1* transgenic lines and mutants after chilling treatment (4°C, 84 h) with ZH10 and DJ as corresponding controls. Mean and stand deviation are given by three independent experiments. ***p < 0.001, from Student's t test.

(legend continued on next page)

independent region. Class 5 stays in the surrounding area and shows a relatively loose relationship to the core region. The 39 diverged-chilling-tolerance-related metabolites are distributed dispersedly in the network, with classes 1–4 as an aggregation region, implying its potential as the core for the regulation network responsible for rice chilling tolerance divergence (Figure 4).

The vitamin E-vitamin K1 sub-network is downstream of COLD1 signaling

A QTL with *COLD1* being the responsible gene is known to be located in the NIP genomic segments in CSSL4-1 (Ma et al., 2015; Figure S1C). We, therefore, focused on *COLD1*, although we could not rule out the possibility that other genes in this genomic region also contribute to the higher chilling tolerance of CSSL4-1. The contribution of *COLD1* to chilling tolerance was confirmed with an analysis of its transgenic plant materials. The *COLD1^{jap}* (haplotype for *japonica*)-overexpression lines exhibit a higher survival rate than wild-type control Zhonghua 10 (ZH10) (57.7% versus 24.5%) with chilling treatment, whereas loss-of-function mutant *cold1-1* exhibited a significantly lower survival rate than corresponding control Dongjin (DJ) (58.4% versus 84.7%) (Figures 5A, 5B, S5A, and S5B).

Given that *COLD1* encodes a membrane protein sensing cold signal, we hypothesized that it might serve to initiate the downstream response of vitamins E and K1 biosynthetic pathways (Ma et al., 2015). Thus, we examined metabolite concentration and gene expression for the transgenic plant materials of *COLD1*. Under chilling treatment, the α -tocopherol level was higher in the *COLD1^{jap}*-overexpression line but lower in *cold1-1*, compared with that in the control (Figure 5C). The overexpression and loss-of-function mutants for *VTE4*, the gene responsible for α -tocopherol biosynthesis, showed increased and decreased chilling tolerance, respectively, confirming its role in cold signaling (Figures S5E–S5J). The expression of *VTE4* was elevated in *COLD1^{jap}*OX8 and suppressed in *cold1-1* compared with the wild-type control, consistent with the change of α -tocopherol (Figures 5C and 5D). Similarly, the level of phylloquinone was higher in *COLD1^{jap}*OX8, but at similar level in *cold1-1* as in the control, probably due to some kind of compensatory mechanism (Figure 5C). *VKORC1*, the key gene in the vitamin K1 pathway, also showed increased expression in *COLD1^{jap}*OX8, but decreased expression in *cold1-1* under chilling stress (Figure 5D; Furt et al., 2010). These data suggest that the vitamin E-vitamin K1 sub-network is downstream of *COLD1*.

COLD1 interacts with G protein α subunit to activate the calcium channel for cold sensing (Ma et al., 2015). To analyze whether the vitamin E-vitamin K1 sub-network is regulated by a calcium signal, we blocked the calcium channel with

lanthanum chloride and checked the chilling response of genes involved in these pathways (Rentel and Knight, 2004). The response for most genes, including *VTE4* and *VKORC1*, were obviously weakened, suggesting that the vitamin E-vitamin K1 sub-network is regulated by calcium signaling at the transcriptional level (Figure S6). This is in accordance with the above conclusion that they are downstream of *COLD1*. Two of these genes showed an unchanged or even stronger chilling response, implying there exists a more complicated regulation mechanism (Figure S6).

The production of α -tocopherol is in connection with chlorophyll metabolism (Gutbrod et al., 2019). The CSSL4-1 is greener than 93-11 when exposed to low environmental temperature in the field (Figure S7). Consistently, *cold1-1* growing under unfavorable illumination also showed decreased chlorophyll content when exposed to chilling treatment, and could be recovered to a nearly normal level through overexpressing *COLD1* (Figures 5E, 5F, S5C, and S5D). These data suggest that similar metabolic pathways are modulated in CSSL4-1 and *cold1-1*, and *COLD1* is probably one of the major genes responsible for the higher chilling tolerance of CSSL4-1.

DISCUSSION

Low environmental temperature limits plant growth and distribution. Rice, as a plant with tropical origination, has evolved a complicated chilling-response network, for which the component sensing cold signal, namely, *COLD1*, has been identified, but its downstream signaling remains unknown (Ma et al., 2015). Our study identified the vitamin E-vitamin K1 sub-network, located in the chloroplast, as the downstream pathway for *COLD1*. Moreover, this sub-network has been proven to be responsible for chilling tolerance divergence, with tocopherol, one form of vitamin E, mediating further chloroplast-nucleus retrograde signaling (Fang et al., 2019). Membrane protein *COLD1*, the vanguard of the cold response system, probably possesses many downstream pathways responsible for different aspects of cold response. Taking advantage of integrated global analysis and the CSSLs between *japonica* and *indica* varieties with clearly different abilities to tolerate chilling stress, our study revealed one of the cold response pathways downstream of *COLD1*, which is crucial for chilling tolerance divergence (Figure 6).

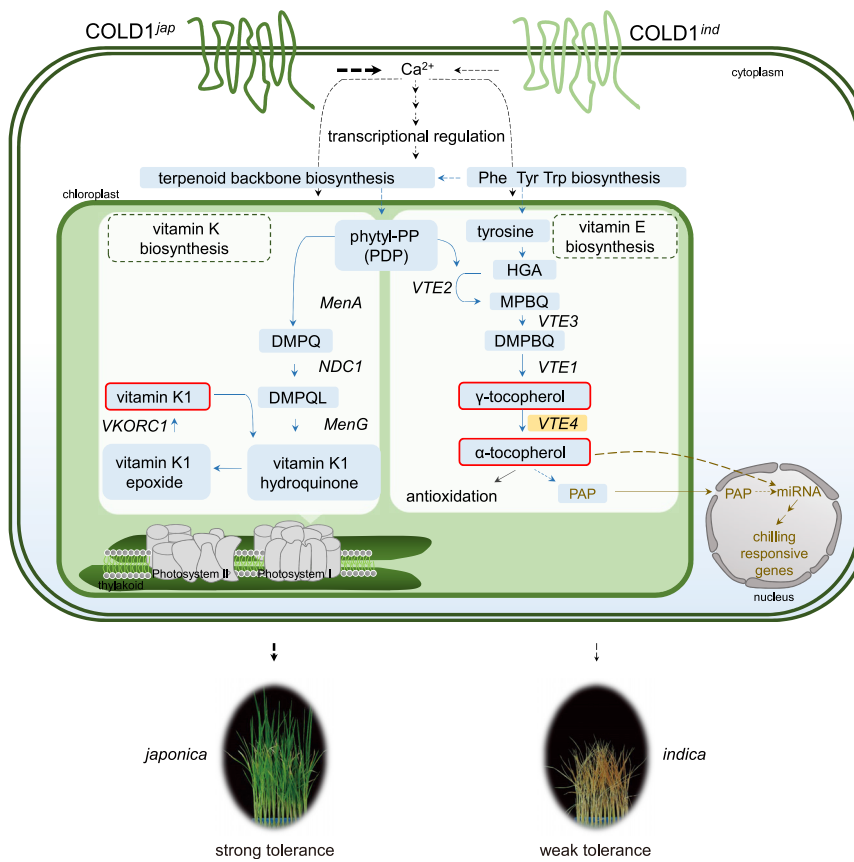
The identification of vitamin E-vitamin K1 sub-network underlying chilling tolerance divergence

The pathway responsible for diverged chilling tolerance was revealed at the transcriptional level. The vitamin E-vitamin K1

(C) Change of concentration (fold change relative to untreated control) for α -tocopherol (vitamin E) and phylloquinone (vitamin K1) in *COLD1^{jap}*OX8 and *cold1-1* mutant under chilling treatment (4°C, 84 h) with ZH10 and DJ as corresponding controls. Mean and stand deviation are given by at least three independent experiments. * $p < 0.05$, ** $p < 0.01$, *** $p < 0.001$; from Student's t test.

(D) Change of the expression (fold change relative to untreated control) for *VTE4* and *VKORC1* in *COLD1^{jap}*OX8 and *cold1-1* mutant under chilling treatment (4°C, 10 h) were measured with quantitative RT-PCR, with ZH10 and DJ as corresponding controls. *ACTIN* was included as the reference gene. Mean and stand deviation are given by at least three independent experiments. ** $p < 0.01$, from Student's t test.

(E and F) The phenotype and chlorophyll content measurement for *COLD1^{jap}*OX8, *cold1-1* and its *COLD1^{jap}*-complemented line, *COLD1^{jap}-OE/cold1-1* L1, with ZH10 and DJ as corresponding controls. Mean and stand deviation are given by at least three independent experiments. ** $p < 0.01$, from Student's t test. Bar, 5 cm.



DEHYDROGENASE C1; MenG, demethylphyloquinol methyltransferase; VKORC1, vitamin-K-epoxide reductase complex subunit 1; VTE1, tocopherol cyclase; VTE2, homogentisic acid phytoltransferase/homogentisate geranylgeranyltransferase; VTE3, MPBQ/2-methyl-6-solanyl-1,4-benzoquinone methyltransferase; VTE4, γ -tocopherol methyltransferase.

sub-network was first outlined through KEGG analysis of genes exhibiting similar change patterns in transcriptomic profiling between substitution line CSSL4-1 and its chilling-tolerant parent line NIP and then confirmed with a similar analysis at the metabolomic level (Figures 2C, 3C, and 3D). The co-expression network of chilling-responsive genes and metabolites further uncovered the central role of vitamin E and vitamin K1, as well as their close connection with photosynthesis (Figure 4).

Vitamin E is a lipid-soluble antioxidant protecting against membrane lipid peroxidation, with α -tocopherol being the highest biologically active form (Muñoz and Munné-Bosch, 2019). There are also reports for its role in photoassimilation and stress tolerance in plants (Hofius et al., 2004; Maeda et al., 2006; Munné-Bosch, 2005; Munné-Bosch et al., 2007). Vitamin K1 (phyloquinone), a membrane-anchored naphthoquinone, functions as an electron carrier in photosystem I (Basset et al., 2017). Our results not only uncovered the function of vitamin E and vitamin K1 in chilling response but also outlined their roles in mediating diverged chilling tolerance between *japonica* and *indica* (Figures 2C, 3C, and 3D). Both vitamin E and vitamin K1 belong to the prenylquinone family. They are mainly synthesized in the chloroplast, and their biosynthetic pathways form a sub-network, which is responsible for *japonica-indica* chilling toler-

Figure 6. Schematic diagram of the possible signaling pathway underlying chilling tolerance divergence between *japonica* and *indica*

In chilling stress, the cold signal is first sensed by COLD1, which affects calcium influx. Calcium signals activate components involved in the vitamin E-vitamin K1 sub-network in the chloroplast, such as VTE4 and VKORC1, through stimulating their gene transcription or other possible ways. Vitamin E functions as a node regulator initiating further downstream cold responses, such as PAP-mediated miRNA biogenesis regulation. *Japonica* and *indica* possess distinct cold sensors and different types of regulation modes, resulting in divergent chilling tolerance. Broken-line arrows, postulated regulation; thick-line arrow, induction of chilling stress response. Metabolites are colored with blue background, and metabolic pathways are outlined with blue arrows. Metabolites involved in chilling tolerance divergence are colored with red border. Yellow cell represents a gene possessing nonsynonymous SNPs that is different between *japonica* and *indica*. Details are shown in Table S7. Arrows and words in brown denote signaling pathway reported in Fang et al. (2019).

COLD1^{jap}, haplotype for *japonica*; COLD^{ind}, haplotype for *indica*; DMPBQ, 2,3-dimethyl-5-phytyl-1,4-benzoquinone; DMPQL, demethyl-phyloquinol; DMPQ, demethyl-phyloquinone; HGA, homogentisic acid; MPBQ, 2-methyl-6-phytyl-1,4-benzoquinone; PAP, 3'-phosphoadenosine 5'-phosphate; phytyl-PP, phytyl pyrophosphate; MenA, 2-carboxy-1,4-naphthoquinone phytoltransferase; NDC1, NAD(P)H

ance divergence, as indicated by transcriptomic, metabolomic, and combined analysis (Figures 2C, 3C, 3D, and 4).

Uncovering cold sensor COLD1 as an upstream regulator for the vitamin E-vitamin K1 sub-network

COLD1, a gene encoding a sensor for low environmental temperature in rice, is located in NIP insertion fragments in CSSL4-1 (Figure S1C). Although COLD1 is known to contain a SNP contributing to *japonica-indica* chilling tolerance divergence, its downstream regulation mechanism is still unclear (Ma et al., 2015). A correlation between chlorophyll loss and tocopherol production has been reported (Gramegna et al., 2019). Both CSSL4-1 and *cold1-1* exhibited a change in chlorophyll content, suggesting that probably the same metabolic pathway was modified in these plant materials (Figures 5E, 5F, and S7). The vitamin E-vitamin K1 synthetic pathway, thus, may be the downstream regulon of COLD1.

To determine whether the vitamin E-vitamin K1 synthetic pathway is under the regulation of COLD1, the concentration of α -tocopherol and the transcription of its biosynthesis gene VTE4 were analyzed for transgenic plants of COLD1 (Bergmüller et al., 2003). The results showed that both α -tocopherol and its regulating gene VTE4 were induced in the overexpression line

but suppressed in the knock-out mutant, consistent with their increased and decreased chilling tolerance (Figures 5A–5D). Similar results were also obtained for the content of phylloquinone and its biosynthetic gene, *VKORC1*, although some kind of compensating mechanism was observed (Figures 5C and 5D; Furt et al., 2010). These data suggest that the vitamin E-vitamin K1 sub-network is under the control of COLD1. COLD1 mediates the cold response through calcium signaling (Ma et al., 2015). We, thus, blocked calcium channel and found that most genes in the vitamin E-vitamin K1 sub-network showed a weakened chilling response, implying that they are regulated by calcium signaling, which is probably mediated by COLD1, in chilling stress.

Among all these signaling pathways downstream of COLD1, the vitamin E-vitamin K1 sub-network is highlighted in our study, probably due to the phenotypes we are interested in and the selection of our research objective. Further studies are needed to reveal more downstream pathways and compare their contribution to the ultimate phenotype.

Chloroplast: an organelle critical for chilling tolerance divergence with retrograde signaling

Our study detecting the mechanism underlying diverged chilling tolerance drew attention to the chloroplast, an organelle acting as an environmental sensor and modulating the expression of thousands of genes in response to environmental stress (Chan et al., 2016). The chloroplast is the organelle in which the vitamin E-vitamin K1 sub-network is localized. Vitamin K1 belongs to photosystem I. The α -tocopherol, closely attached to the lipid bilayer of thylakoids or the inner chloroplast envelope, plays a role in photoprotection (Havaux et al., 2005; Muñoz and Munné-Bosch, 2019). This is consistent with the results of metabolomic and transcriptomic co-expression network analysis, which indicates that the function of vitamin E is closely related to photosynthesis in cold stress response (Figure 4).

The chloroplast is very sensitive to environmental signals, and photosynthesis belongs to the first group of biological processes influenced by temperature fluctuation (Hüner et al., 2012; Mathur et al., 2014). Disturbance of photosynthesis results in the formation of reactive oxygen species (ROS) (Chan et al., 2016). Vitamin E helps to eliminate ROS, and α -tocopherol is a nonenzymatic antioxidant, which modulates the redox state of the chloroplast and affects retrograde signaling from the chloroplast (Dong et al., 2019; Havaux et al., 2005; Krieger-Liszka and Trebst, 2006). Recently, another tocopherol-mediated chloroplast-to-nucleus signaling pathway has also been reported, in which tocopherol regulates the production of its downstream metabolite 3'- phosphoadenosine 5'- phosphate (PAP), which regulates microRNA (miRNA) biogenesis in the nucleus (Fang et al., 2019). Tocopherol, modulating or being modulated by multiple phytohormones, is the node of multiple signaling pathways, and not surprisingly, it is selected as the regulating site for adaptation to different environmental temperatures (Allu et al., 2017; Jiang et al., 2017; Sereflioglu et al., 2017).

According to our results, a signaling pathway, ranging from membrane protein to chloroplast and then to the nucleus, has been outlined, although some gaps still exist. The cold signal is first sensed by membrane protein COLD1, which triggers the

influx of calcium, a ubiquitous intracellular second messenger. Calcium signals activate components involved in the vitamin E-vitamin K1 sub-network, possibly through stimulating their gene transcription or other possible pathways (Kudla et al., 2018; Navazio et al., 2020). Vitamin E functions as a node regulator initiating further downstream cold responses, including activating chloroplast-nucleus retrograde signaling mediated by its downstream metabolite PAP (Fang et al., 2019; Navazio et al., 2020; Stael, 2019; Wang et al., 2019b). *Japonica* and *indica* possess different type of cold sensors and probably different kinds of regulation modes, which results in their differential ability to tolerate chilling stress (Figure 6). Of course, further study is needed to analyze how the vitamin E-vitamin K1 sub-network is activated by the calcium signal in chilling response and to identify more plant cold sensors besides COLD1. Our study has uncovered that the vitamin E-vitamin K1 sub-network, downstream of COLD1, is responsible for chilling tolerance divergence with the aid of genetic population and integrated transcriptomic and metabolomic analysis, revealing the regulation point of the cold response system in rice. These results may have great potential for rice cold tolerance improvement through molecular breeding.

STAR★METHODS

Detailed methods are provided in the online version of this paper and include the following:

- KEY RESOURCES TABLE
- RESOURCE AVAILABILITY
 - Lead contact
 - Materials availability
 - Data and code availability
- EXPERIMENTAL MODEL AND SUBJECT DETAILS
- METHOD DETAILS
 - Plant material and chilling treatment
 - RNA-Seq
 - Metabolomic profiling
 - Data analysis
 - Quantitative RT-PCR
 - Tocopherol extraction and analysis
 - Chlorophyll measurement
 - Lanthanum chloride treatment
- QUANTIFICATION AND STATISTICAL ANALYSIS

SUPPLEMENTAL INFORMATION

Supplemental information can be found online at <https://doi.org/10.1016/j.celrep.2021.109397>.

ACKNOWLEDGMENTS

We thank Guohua Liang (Yangzhou University, China) for providing CSSL materials and Lining Guo (Metabolon) for his help and useful comments about metabolomic analysis. This work was supported by the Strategic Priority Research Program of the Chinese Academy of Sciences (grant no. XDB27040104) and the National Natural Science Foundation of China (grant no. 32070294).

AUTHOR CONTRIBUTIONS

W.L., Q.H., Y.X., K.C., and J.Z. designed the experiments; W.L. and J.Z. performed the experiments; Q.H. and J.Z. analyzed the data; W.L., Q.H., W.Q., and J.Z. wrote the manuscript. All authors read and approved the final manuscript.

DECLARATION OF INTERESTS

The authors declare no competing interests.

INCLUSION AND DIVERSITY

The author list of this paper includes contributors from the location where the research was conducted who participated in the data collection, design, analysis, and/or interpretation of the work.

Received: November 30, 2020

Revised: April 30, 2021

Accepted: June 22, 2021

Published: July 20, 2021

REFERENCES

- Allu, A.D., Simancas, B., Balazadeh, S., and Munné-Bosch, S. (2017). Defense-related transcriptional reprogramming in vitamin E-deficient *Arabidopsis* mutants exposed to contrasting phosphate availability. *Front. Plant Sci.* 8, 1396.
- Anders, S., Pyl, P.T., and Huber, W. (2015). HTSeq—a Python framework to work with high-throughput sequencing data. *Bioinformatics* 31, 166–169.
- Basset, G.J., Latimer, S., Fatihi, A., Soubeiran, E., and Block, A. (2017). Phylloquinone (Vitamin K1): occurrence, biosynthesis and functions. *Mini Rev. Med. Chem.* 17, 1028–1038.
- Bergmüller, E., Porfirova, S., and Dörmann, P. (2003). Characterization of an *Arabidopsis* mutant deficient in gamma-tocopherol methyltransferase. *Plant Mol. Biol.* 52, 1181–1190.
- Chan, K.X., Phua, S.Y., Crisp, P., McQuinn, R., and Pogson, B.J. (2016). Learning the languages of the chloroplast: retrograde signaling and beyond. *Annu. Rev. Plant Biol.* 67, 25–53.
- Chen, R., Feldstein, A.E., and McIntyre, T.M. (2009). Suppression of mitochondrial function by oxidatively truncated phospholipids is reversible, aided by bid, and suppressed by Bcl-XL. *J. Biol. Chem.* 284, 26297–26308.
- Cuevas, J.C., López-Cobollo, R., Alcázar, R., Zarza, X., Koncz, C., Altabella, T., Salinas, J., Tiburcio, A.F., and Ferrando, A. (2008). Putrescine is involved in *Arabidopsis* freezing tolerance and cold acclimation by regulating abscisic acid levels in response to low temperature. *Plant Physiol.* 148, 1094–1105.
- Dong, Q., Zhang, Y.X., Zhou, Q., Liu, Q.E., Chen, D.B., Wang, H., Cheng, S.H., Cao, L.Y., and Shen, X.H. (2019). UMP kinase regulates chloroplast development and cold response in rice. *Int. J. Mol. Sci.* 20, 2107.
- Evans, A.M., DeHaven, C.D., Barrett, T., Mitchell, M., and Milgram, E. (2009). Integrated, nontargeted ultrahigh performance liquid chromatography/electrospray ionization tandem mass spectrometry platform for the identification and relative quantification of the small-molecule complement of biological systems. *Anal. Chem.* 81, 6656–6667.
- Fang, X., Zhao, G., Zhang, S., Li, Y., Gu, H., Li, Y., Zhao, Q., and Qi, Y. (2019). Chloroplast-to-Nucleus signaling regulates microRNA biogenesis in *Arabidopsis*. *Dev. Cell* 48, 371–382.e4.
- Furt, F., Oostende, Cv., Widhalm, J.R., Dale, M.A., Wertz, J., and Basset, G.J. (2010). A bimodular oxidoreductase mediates the specific reduction of phylloquinone (vitamin K₁) in chloroplasts. *Plant J.* 64, 38–46.
- Ge, L., Chen, H., Jiang, J.F., Zhao, Y., Xu, M.L., Xu, Y.Y., Tan, K.H., Xu, Z.H., and Chong, K. (2004). Overexpression of *OsRAA1* causes pleiotropic phenotypes in transgenic rice plants, including altered leaf, flower, and root development and root response to gravity. *Plant Physiol.* 135, 1502–1513.
- Gramegna, G., Rosado, D., Sánchez Carranza, A.P., Cruz, A.B., Simon-Moya, M., Llorente, B., Rodríguez-Concepción, M., Freschi, L., and Rossi, M. (2019). PHYTOCHROME-INTERACTING FACTOR 3 mediates light-dependent induction of tocopherol biosynthesis during tomato fruit ripening. *Plant Cell Environ.* 42, 1328–1339.
- Guo, X., Liu, D., and Chong, K. (2018). Cold signaling in plants: Insights into mechanisms and regulation. *J. Integr. Plant Biol.* 60, 745–756.
- Gutaker, R.M., Groen, S.C., Bellis, E.S., Choi, J.Y., Pires, I.S., Bocinsky, R.K., Slayton, E.R., Wilkins, O., Castillo, C.C., Negrão, S., et al. (2020). Genomic history and ecology of the geographic spread of rice. *Nat. Plants* 6, 492–502.
- Gutbrod, K., Romer, J., and Dörmann, P. (2019). Phytol metabolism in plants. *Prog. Lipid Res.* 74, 1–17.
- Hashida, S.N., Takahashi, H., and Uchimiya, H. (2009). The role of NAD biosynthesis in plant development and stress responses. *Ann. Bot.* 103, 819–824.
- Havaux, M., Eymery, F., Porfirova, S., Rey, P., and Dörmann, P. (2005). Vitamin E protects against photoinhibition and photooxidative stress in *Arabidopsis thaliana*. *Plant Cell* 17, 3451–3469.
- Hofius, D., Hajirezaei, M.R., Geiger, M., Tschiersch, H., Melzer, M., and Sonnewald, U. (2004). RNAi-mediated tocopherol deficiency impairs photoassimilate export in transgenic potato plants. *Plant Physiol.* 135, 1256–1268.
- Hullin-Matsuda, F., Makino, A., Murate, M., and Kobayashi, T. (2016). Probing phosphoethanolamine-containing lipids in membranes with duramycin/cinnamycin and aegerolysin proteins. *Biochimie* 130, 81–90.
- Hüner, N.P., Bode, R., Dahal, K., Hollis, L., Rosso, D., Krol, M., and Ivanov, A.G. (2012). Chloroplast redox imbalance governs phenotypic plasticity: the “grand design of photosynthesis” revisited. *Front. Plant Sci.* 3, 255.
- Jayaram, H.N., Kusumanchi, P., and Yalowitz, J.A. (2011). NMNAT expression and its relation to NAD metabolism. *Curr. Med. Chem.* 18, 1962–1972.
- Jiang, Q., Xu, T., Huang, J., Jannasch, A.S., Cooper, B., and Yang, C. (2015). Analysis of vitamin E metabolites including carboxychromanols and sulfated derivatives using LC/MS/MS. *J. Lipid Res.* 56, 2217–2225.
- Jiang, J., Chen, Z., Ban, L., Wu, Y., Huang, J., Chu, J., Fang, S., Wang, Z., Gao, H., and Wang, X. (2017). P-HYDROXYPHENYL PYRUVATE DIOXYGENASE from *Medicago sativa* is involved in vitamin E biosynthesis and abscisic acid-mediated seed germination. *Sci. Rep.* 7, 40625.
- Kawahara, Y., de la Bastide, M., Hamilton, J.P., Kanamori, H., McCombie, W.R., Ouyang, S., Schwartz, D.C., Tanaka, T., Wu, J., Zhou, S., et al. (2013). Improvement of the *Oryza sativa* Nipponbare reference genome using next generation sequence and optical map data. *Rice (N. Y.)* 6, 4.
- Kim, D., Langmead, B., and Salzberg, S.L. (2015). HISAT: a fast spliced aligner with low memory requirements. *Nat. Methods* 12, 357–360.
- Körner, C. (2016). Plant adaptation to cold climates. *F1000Res* 5, F1000 Faculty Rev-2769.
- Kosma, D.K., Rice, A., and Pollard, M. (2015). Analysis of aliphatic waxes associated with root periderm or exodermis from eleven plant species. *Phytochemistry* 117, 351–362.
- Krieger-Liszskay, A., and Trebst, A. (2006). Tocopherol is the scavenger of singlet oxygen produced by the triplet states of chlorophyll in the PSII reaction centre. *J. Exp. Bot.* 57, 1677–1684.
- Kudla, J., Becker, D., Grill, E., Hedrich, R., Hippler, M., Kummer, U., Parniske, M., Romeis, T., and Schumacher, K. (2018). Advances and current challenges in calcium signaling. *New Phytol.* 218, 414–431.
- Kumar, S., Stecher, G., and Tamura, K. (2016). MEGA7: Molecular evolutionary genetics analysis version 7.0 for bigger datasets. *Mol. Biol. Evol.* 33, 1870–1874.
- Langfelder, P., and Horvath, S. (2008). WGCNA: an R package for weighted correlation network analysis. *BMC Bioinformatics* 9, 559.
- Langmead, B., and Salzberg, S.L. (2012). Fast gapped-read alignment with Bowtie 2. *Nat. Methods* 9, 357–359.
- Liu, C., Ou, S., Mao, B., Tang, J., Wang, W., Wang, H., Cao, S., Schläppi, M.R., Zhao, B., Xiao, G., et al. (2018). Early selection of *bZIP73* facilitated adaptation of *japonica* rice to cold climates. *Nat. Commun.* 9, 3302.

- Ma, Y., Dai, X., Xu, Y., Luo, W., Zheng, X., Zeng, D., Pan, Y., Lin, X., Liu, H., Zhang, D., et al. (2015). *COLD1* confers chilling tolerance in rice. *Cell* 160, 1209–1221.
- Maeda, H., Song, W., Sage, T.L., and DellaPenna, D. (2006). Tocopherols play a crucial role in low-temperature adaptation and Phloem loading in *Arabidopsis*. *Plant Cell* 18, 2710–2732.
- Manishankar, P., and Kudla, J. (2015). Cold tolerance encoded in one SNP. *Cell* 160, 1045–1046.
- Mao, D., Yu, H., Liu, T., Yang, G., and Xing, Y. (2011). Two complementary recessive genes in duplicated segments control etiolation in rice. *Theor. Appl. Genet.* 122, 373–383.
- Mao, D., Xin, Y., Tan, Y., Hu, X., Bai, J., Liu, Z.Y., Yu, Y., Li, L., Peng, C., Fan, T., et al. (2019). Natural variation in the *HAN1* gene confers chilling tolerance in rice and allowed adaptation to a temperate climate. *Proc. Natl. Acad. Sci. USA* 116, 3494–3501.
- Mathur, S., Agrawal, D., and Jajoo, A. (2014). Photosynthesis: response to high temperature stress. *J. Photochem. Photobiol. B* 137, 116–126.
- Mène-Saffrané, L. (2017). Vitamin E biosynthesis and its regulation in plants. *Antioxidants* 7, 2.
- Moon, S.J., Min, M.K., Kim, J.A., Kim, D.Y., Yoon, I.S., Kwon, T.R., Byun, M.O., and Kim, B.G. (2019). Ectopic expression of *OsDREB1G*, a member of the Os-DREB1 Subfamily, confers cold stress tolerance in rice. *Front. Plant Sci.* 10, 297.
- Munné-Bosch, S. (2005). The role of alpha-tocopherol in plant stress tolerance. *J. Plant Physiol.* 162, 743–748.
- Munné-Bosch, S., Weiler, E.W., Alegre, L., Müller, M., Düchting, P., and Falk, J. (2007). Alpha-tocopherol may influence cellular signaling by modulating jasmonic acid levels in plants. *Planta* 225, 681–691.
- Muñoz, P., and Munné-Bosch, S. (2019). Vitamin E in plants: biosynthesis, transport, and function. *Trends Plant Sci.* 24, 1040–1051.
- Navazio, L., Formentin, E., Cendron, L., and Szabó, I. (2020). Chloroplast calcium signaling in the spotlight. *Front. Plant Sci.* 11, 186.
- Noctor, G., Mhamdi, A., Chaouch, S., Han, Y., Neukermans, J., Marquez-Garcia, B., Queval, G., and Foyer, C.H. (2012). Glutathione in plants: an integrated overview. *Plant Cell Environ.* 35, 454–484.
- Ohkama-Ohtsu, N., Okawa, A., Zhao, P., Xiang, C., Saito, K., and Oliver, D.J. (2008). A gamma-glutamyl transpeptidase-independent pathway of glutathione catabolism to glutamate via 5-oxoproline in *Arabidopsis*. *Plant Physiol.* 148, 1603–1613.
- Rentel, M.C., and Knight, M.R. (2004). Oxidative stress-induced calcium signaling in *Arabidopsis*. *Plant Physiol.* 135, 1471–1479.
- Rodrigues, N., Malheiro, R., Casal, S., Asensio-S-Manzanera, M.C., Bento, A., and Pereira, J.A. (2012). Influence of spike lavender (*Lavandula latifolia* Med.) essential oil in the quality, stability and composition of soybean oil during microwave heating. *Food Chem.* 50, 2894–2901.
- Sakai, H., Lee, S.S., Tanaka, T., Numa, H., Kim, J., Kawahara, Y., Wakimoto, H., Yang, C.C., Iwamoto, M., Abe, T., et al. (2013). Rice Annotation Project Database (RAP-DB): an integrative and interactive database for rice genomics. *Plant Cell Physiol.* 54, e6.
- Sánchez-Migallón, M.P., Aranda, F.J., and Gómez-Fernández, J.C. (1996). Interaction between alpha-tocopherol and heteroacid phosphatidylcholines with different amounts of unsaturation. *Biochim. Biophys. Acta* 1279, 251–258.
- Sereflioglu, S., Dinler, B.S., and Tasci, E. (2017). Alpha-tocopherol-dependent salt tolerance is more related with auxin synthesis rather than enhancement antioxidant defense in soybean roots. *Acta Biol. Hung.* 68, 115–125.
- Shannon, P., Markiel, A., Ozier, O., Baliga, N.S., Wang, J.T., Ramage, D., Amin, N., Schwikowski, B., and Ideker, T. (2003). Cytoscape: a software environment for integrated models of biomolecular interaction networks. *Genome Res.* 13, 2498–2504.
- Shi, B., Ni, L., Zhang, A., Cao, J., Zhang, H., Qin, T., Tan, M., Zhang, J., and Jiang, M. (2012). OsDMI3 is a novel component of abscisic acid signaling in the induction of antioxidant defense in leaves of rice. *Mol. Plant* 5, 1359–1374.
- Stael, S. (2019). Chloroplast calcium signalling quenches a thirst. *Nat. Plants* 5, 559–560.
- Storey, J.D. (2012). A direct approach to false discovery rates. *J. R. Stat. Soc. B* 64, 9.
- Verma, S., and Mishra, S.N. (2005). Putrescine alleviation of growth in salt stressed *Brassica juncea* by inducing antioxidative defense system. *J. Plant Physiol.* 162, 669–677.
- Wang, P., Xiong, Y., Gong, R., Yang, Y., Fan, K., and Yu, S. (2019a). A key variant in the cis-regulatory element of flowering gene *Ghd8* associated with cold tolerance in rice. *Sci. Rep.* 9, 9603.
- Wang, Q., Yang, S., Wan, S., and Li, X. (2019b). The significance of calcium in photosynthesis. *Int. J. Mol. Sci.* 20, 1353.
- Xie, C., Mao, X., Huang, J., Ding, Y., Wu, J., Dong, S., Kong, L., Gao, G., Li, C.Y., and Wei, L. (2011). KOBAS 2.0: a web server for annotation and identification of enriched pathways and diseases. *Nucleic Acids Res.* 39, W316–W322.
- Xu, J., Zhao, Q., Du, P., Xu, C., Wang, B., Feng, Q., Liu, Q., Tang, S., Gu, M., Han, B., and Liang, G. (2010). Developing high throughput genotyped chromosome segment substitution lines based on population whole-genome resequencing in rice (*Oryza sativa* L.). *BMC Genomics* 11, 656.
- Yoshida, S., Forno, D.A., Cock, J.H., and Gomez, K.A. (1976). Laboratory manual for physiological studies of rice. (International Rice Research Institute).
- Zhang, J., Luo, W., Zhao, Y., Xu, Y., Song, S., and Chong, K. (2016). Comparative metabolomic analysis reveals a reactive oxygen species-dominated dynamic model underlying chilling environment adaptation and tolerance in rice. *New Phytol.* 211, 1295–1310.
- Zhang, Z., Li, J., Li, F., Liu, H., Yang, W., Chong, K., and Xu, Y. (2017). Os-MAPK3 phosphorylates OsbHLH002/OsICE1 and inhibits its ubiquitination to activate OsTPP1 and enhances rice chilling tolerance. *Dev. Cell* 43, 731–743.e5.
- Zhang, D., Guo, X., Xu, Y., Li, H., Ma, L., Yao, X., Weng, Y., Guo, Y., Liu, C.M., and Chong, K. (2019). OsCIPK7 point-mutation leads to conformation and kinase-activity change for sensing cold response. *J. Integr. Plant Biol.* 61, 1194–1200.

STAR★METHODS

KEY RESOURCES TABLE

REAGENT or RESOURCE	SOURCE	IDENTIFIER
Bacterial and virus strains		
<i>Escheichia coli</i> DH5α	BioMed	Cat# BC102
<i>Agrobacterium tumefaciens</i> EHA105	BioMed	Cat# BC303
Chemicals, peptides, and recombinant proteins		
TRIzol	Invitrogen	Cat# 15596026
M-MLV Reverse Transcriptase	Promega	Cat# M1701
DNA Polymerase I	QIAGEN	Cat# 200203
Phusion High-Fidelity DNA Polymerase	New England Biolabs	Cat# M0530S
SYBR Green Real-time PCR Master mix	Toyobo	Cat# QPK-201
Lanthanum chloride (LaCl_3)	Sigma	Cat# 10099-58-8
Critical commercial assays		
CRISPR/Cas vector construction Kit	Biogel	Cat# BGK03
RNeasy Plant Mini Kit	QIAGEN	Cat# 154041662
Gel Extraction Kit	OMEGA	Cat# D2500-01
Plasmid Mini Kit I	OMEGA	Cat# D6943-01
NEBNEXT® Ultra RNA Library Prep Kit for Illumina®	New England Biolabs	Cat# E7770
AMPure XP system	Beckman Coulter	Cat# A63880
Deposited data		
RNA-seq datasets	This paper	Genome Sequence Archive in National Genomics Data Center: CRA003197 https://ngdc.cncb.ac.cn/gsa/browse/CRA003197 ; the Mendeley Dataset: http://doi.org/10.17632/74pzb35ggj.1
The rice reference genome	IRGSP-1.0	https://rapdb.dna.affrc.go.jp/
Metabolomic datasets	This paper	See Tables S2 and S3
Nucleotide diversity	Rice SNP-Seek Database	https://snp-seek.irri.org/
Raw imaging data	This paper; Mendeley Data	https://doi.org/10.17632/y4vt4xhv7.1
Experimental models: Organisms/strains		
Rice: Nippobare (NIP)	This paper	N/A
Rice: 93-11	This paper	N/A
Rice: CSSL4-1	This paper	N/A
Rice: Chromosome segment lines (CSSLs)	Xu et al., 2010	N/A
Rice: Zhonghua10 (ZH10)	This paper	N/A
Rice: <i>COLD1^{jap}</i> -OX8	This paper	N/A
Rice: Dongjin (DJ)	Ma et al., 2015	N/A
Rice: <i>cold1-1</i>	Ma et al., 2015	N/A
Rice: <i>COLD1^{jap}</i> -OE/ <i>cold1-1</i> L1	Ma et al., 2015	N/A
Rice: Zhonghua11 (ZH11)	This paper	N/A
Rice: <i>VTE4</i> OX16	This paper	N/A
Rice: <i>VTE4</i> OX37	This paper	N/A
Rice: <i>vte4</i> L7	This paper	N/A
Rice: <i>vte4</i> L11	This paper	N/A
Oligonucleotides		
See Table S10 for oligonucleotide information	This paper	N/A

(Continued on next page)

Continued

REAGENT or RESOURCE	SOURCE	IDENTIFIER
Recombinant DNA		
pCRISPR/Cas	Biogle	Cat# BGK03
pUN1301	Ge et al., 2004	N/A
<i>COLD1^{lap}</i> -pUN1301	This paper	N/A
VTE4-pUN1301	This paper	N/A
pCRISPR/Cas-VTE4-sgRNA	This paper	N/A
Software and algorithms		
Bowtie2	Langmead and Salzberg, 2012	http://bowtie-bio.sourceforge.net/bowtie2/index.shtml
HISAT	Kim et al., 2015	http://www.ccb.jhu.edu/software/hisat/index.shtml
HTSeq	Anders et al., 2015	https://htseq.readthedocs.io/en/master/
JMP	SAS	https://wwwjmp.com/
WGCNA R package	Langfelder and Horvath, 2008	https://cran.r-project.org/web/packages/WGCNA/index.html
KOBAS 3.0	Xie et al., 2011	http://bioinfo.org/kobas/
Cytoscape	Shannon et al., 2003	https://cytoscape.org/
MEGA7	Kumar et al., 2016	RRID: SCR_000667, https://megasoftware.net/

RESOURCE AVAILABILITY

Lead contact

Further information and requests for resources and reagents should be directed to and will be fulfilled by the Lead Contact, Jingyu Zhang (jingyuzhang@ibcas.ac.cn).

Materials availability

All unique/stable reagents generated in this study are available from the Lead Contact with a completed Materials Transfer Agreement.

Data and code availability

RNA-seq data reported in this paper have been deposited in the Genome Sequence Archive in National Genomics Data Center (<https://ngdc.cncb.ac.cn/gsa>), under the accession number: CRA003197 (<https://ngdc.cncb.ac.cn/gsa/browse/CRA003197>), also in the Mendeley Dataset under <http://doi.org/10.17632/74pzb35ggj.1>. Metabolomic data is provided in the Tables S2 and S3. Original phenotype images and agarose gel electrophoresis images have been deposited at Mendeley Dataset under <https://doi.org/10.17632/y4vt4xhv7.1>.

EXPERIMENTAL MODEL AND SUBJECT DETAILS

The *Oryza sativa* ssp. *Geng/Japonica* cultivar Nippobare (NIP), Zhonghua10 (ZH10), Zhonghua 11 (ZH11), Dongjin (DJ) and *Oryza sativa* ssp. *Xian/Indica* cultivar 93-11 were used in this study. The chromosome segment substitution lines (CSSLs) generated from NIP and 93-11 were kindly provided by Prof. Guohua Liang (Xu et al., 2010). The T-DNA insertion line PFG_1B-11312 (*cold1-1*) in the Dongjin background was obtained from RiceGE (<http://signal.salk.edu/cgi-bin/RiceGE/>), the Rice Functional Genomics Express Database, in Pohang city, Korea, as described previously (Ma et al., 2015). To test chilling tolerance for NIP, 93-11, CSSL4-1 and *COLD1* transgenic lines, the rice seedling was planted in chamber with nutrient soil under 10 h/14 h light (34827 lux) /dark, light 28–30°C / dark 25°C conditions for 2 weeks, and then transferred into artificial incubator under 10 h /14 h light/dark, at 4°C for 41 hours (NIP, 93-11 and CSSLs), 84 h (ZH10, ZH11, *COLD1^{lap}*OX8, *cold1-1* and *COLD1^{lap}OE/cold1-1 L1*). After chilling treatment, the seedling was transferred back to normal growth conditions for 7 days (NIP, 93-11 and CSSLs) or 14 days (ZH10, ZH11, *COLD1^{lap}*OX8, *cold1-1* and *COLD1^{lap}OE/cold1-1 L1*). To test chilling tolerance for *VTE4* transgenic lines, the rice seedlings were cultured in Yoshida's nutrient solution (Yoshida et al., 1976) under 10 h/14 h light (34827 lux) /dark, light 28–30°C / dark 25°C conditions for 2 weeks, and then transferred into artificial incubator under 10 h /14 h light/dark, at 4°C for 78 hours. After chilling treatment, the seedling was transferred back to normal growth conditions for 14 days. For RNA-Seq, total RNA was extracted from the aerial parts of seedlings with TRIzol (Invitrogen, Carlsbad, CA, USA). Sequencing libraries were generated using NEBNext® Ultra

RNA Library Prep Kit for Illumina® (New England Biolabs, Beverly, MA, USA) and sequenced on the Illumina Hiseq platform. Global unbiased metabolic profiling was performed with the aerial parts of seedlings by Metabolon (<https://www.metabolon.com/>) with three independent platforms, ultra-high-performance liquid chromatography/tandem mass spectrometry (UHLC/MS/MS²), UHLC/MS/MS², gas chromatography/mass spectrometry (GC/MS). Value of each metabolite was calculated as described previously (Evans et al., 2009).

METHOD DETAILS

Plant material and chilling treatment

Nipponbare (NIP, *Oryza sativa*. ssp. *japonica*) and 93-11 (*Oryza sativa*. ssp. *indica*) were used in this study. Chromosome segment substitution lines (CSSLs) population were derived from crossing between NIP and 93-11, and backcrossing with 93-11 for five times at least and self-crossing one time to produced CSSLs (Xu et al., 2010). Chilling treatment was performed as described previously (Ma et al., 2015). After germination, seeds of three varieties (NIP, 93-11 and CSSL4-1) were grown in 20 cm × 20 cm chamber with nutrient soil (day/night: 28–30°C/25°C, 10 hours/14 hours) for about 2 weeks (Figures S5C and S5D). Then, the seedlings at the stage of three leaves were exposed to chilling treatment at 4°C ± 0.5°C in the artificial climate chamber for two time-points, 10 hours and 41 hours. Finally, each group of rice seedlings was moved to the glasshouse and grown for another 3 days to recovery, and the aerial parts of rice seedlings were harvested. Untreated controls at similar growth stage were also harvested at each time point to eliminate the growth effect. All these materials were used to perform mRNA sequencing or metabolism profiling. Wilted phenotype and survival rate (live seedling number divided by total tested seedling number) were recorded after recovery for 7 days. Each experiment was biologically repeated at least three times.

The overexpression line of *COLD1^{lap}* (haplotype for *japonica*, *COLD1^{lap}OX8*) and *VTE4* (*VTE4OX*) were acquired through gene transformation as described previously (Ge et al., 2004). Briefly, the CDS sequence of *COLD1^{lap}* and *VTE4* were amplified from NIP and inserted into the pUN1301 vector. Plasmids were transformed into the *japonica* cultivar Zhonghua10 (ZH10) or Zhonghua11 (ZH11). On the other hand, *cold1-1*, T-DNA insertion mutant for *COLD1* with Dongjin (DJ, *japonica* cultivar) background was bought from the Korea Rice Mutant Center (Pohang, Korea), as described previously (Ma et al., 2015). The mutant for *VTE4*, *vte4*, was generated with CRISPR/Cas9 with ZH10 background (Biogle Co. Ltd. Hangzhou, China). Chilling treatment was performed as described above, but the duration of treatment was modified according to different genetic backgrounds. *COLD1^{lap}OX8* (with ZH10 background), *cold1-1* (with DJ background), and their corresponding wild-type were subjected to chilling treatment for 84 hours, then recovered for 3 days for α-tocopherol measurement, or 14 days for survival rate analysis. For *VTE4OX* (with ZH11 background), *vte4* (with ZH10 background), and their wild-type control, chilling treatment was performed at 4°C for 84 hours and recovered for 14 days. Then, phenotype recording and survival rate analysis were performed. Each experiment was biologically repeated at least three times. The primers used for vector construction are listed in Table S10.

RNA-Seq

Total RNA was extracted from the aerial parts of seedlings with TRIzol (Invitrogen, Carlsbad, CA, USA). Sequencing libraries were generated using NEBNext® Ultra RNA Library Prep Kit for Illumina® (New England Biolabs, Beverly, MA, USA). Briefly, mRNA was purified from total RNA using poly-T oligo-attached magnetic beads. First strand cDNA was synthesized using random hexamer primer and M-MLV Reverse Transcriptase (RNase H). Second strand cDNA synthesis was performed using DNA Polymerase I and RNase H. The library fragments were obtained and purified with AMPure XP system (Beckman Coulter, Beverly, MA, USA). PCR amplification was performed with Phusion High-Fidelity DNA Polymerase (New England Biolabs, Beverly, MA, USA), then sequenced on the Illumina Hiseq platform.

Metabolomic profiling

The global unbiased metabolic profiling was performed by Metabolon (<https://www.metabolon.com/>) with three independent platforms, ultra-high-performance liquid chromatography/tandem mass spectrometry (UHLC/MS/MS²), UHLC/MS/MS², gas chromatography/mass spectrometry (GC/MS). Five biological replicates was performed for most samples, except for a few four replicates. Compounds were identified by comparing the ion features with a reference library. Artificial peaks were removed with process blanks (water only) and solvent blanks. Value of each metabolite was calculated as described previously (Evans et al., 2009). For better data visualization, the raw count for each metabolite was rescaled through diving each sample value by the median value for this specific metabolite, as described previously (Zhang et al., 2016)

Data analysis

For mRNA sequencing, clean reads of RNA-Seq were aligned to reference genome (Os-Nipponbare-Reference-IRGSP-1.0; <https://rapdb.dna.affrc.go.jp/>; Kawahara et al., 2013; Sakai et al., 2013). Index of the reference genome was built using Bowtie2 and clean reads were aligned to the reference genome using HISAT (Langmead and Salzberg, 2012; Kim et al., 2015). The gene expression level was estimated using HTSeq (Anders et al., 2015). Genes which showed absolute value of log₂ fold change ≥ 1 after chilling treatment in both CSSL4-1 and NIP, but < 1 in 93-11 were selected as candidates responsible for *japonica-indica* chilling divergence.

For metabolomic profiling, JMP (SAS; <https://www.jmp.com/>) and an R package (<http://cran.r-project.org/>) were used for statistical analysis. The relative metabolic level was calculated as the ratio of scaled amount of chilling-treated sample compared with that of untreated sample. Significant ($p < 0.05$) increase or decrease was determined by Welch's two-sample t test. Q value was used to estimate false discovery rate (FDR) (Storey, 2012; Tables S2 and S3). The candidates responsible for chilling tolerance divergence were defined as metabolites whose \log_2 -transformation value showing difference smaller than 0.5 between CSSL4-1 and NIP, but larger than 0.5 between CSSL4-1 and 93-11 under either mild or severe chilling treatment, also with at least \log_2 fold change ≥ 0.263 or ≤ -0.263 in NIP after chilling treatment.

For weighted correlation network analysis, soft-thresholding powers were calculated by R Package (Figures S4A and S4B; Langfelder and Horvath, 2008). The network was shown by cytoscape software (Shannon et al., 2003). The Kyoto Encyclopedia of Genes and Genomes (KEGG) pathway analysis was performed by KOBAS 3.0 (<http://bioinfo.org/kobas/>), eliminating genes without corresponding IDs (Xie et al., 2011). Genes exposed to further analysis were selected according to the KEGG database.

Quantitative RT-PCR

Quantitative RT-PCR (qRT-PCR) were performed as described previously (Ma et al., 2015). Total RNA was extracted with RNeasy Plant Mini Kit (QIAGEN, Germantown, MD, USA), transcribed by M-MLV reverse transcriptase (Promega, USA) with RNase free DNase I (QIAGEN, Valencia, CA, USA). SYBR Green Real-time PCR Master mix (Toyobo, Osaka, Japan) was carried out using an MX3000P real-time PCR system (Stratagene, USA). ACTIN was included as the reference gene. Relative quantification ($\Delta\text{-}\Delta\text{CT}$) was employed to measure quantitative variation between replicates. Primers used are listed in the Table S10.

Tocopherol extraction and analysis

Tocopherol was extracted and analyzed with LC-MS/MS (Jiang et al., 2015; Rodrigues et al., 2012). 0.05 g samples at the three-leaf stage were ground with 800 μL n-hexane/acetic ether 85:15 (V/V) buffer, then centrifuged at 25000 $\times g$ for 20 min (4°C). 500 μL upper layer was transferred into a separate tube. Standard sample (vitamin E, 1 mg/ml) was dilute into 20 ppb, 50 ppb, 100 ppb, 200 ppb, 500 ppb, 1 ppm, 2 ppm, and 4 ppm by n-hexane/acetic ether 85:15 (V/V) buffer and the volume was 1 ml. 500 μL standard samples with various concentration were unwater in freeze dryer and added 100 μL 100% acetonitrile, and centrifugation (4°C, 25000 $\times g$, 20 min). The upper layer was transferred into a separate tube. Tocopherol was analyzed by LC-MS/MS (SCIEX ExionLC and AB SCIEX QTRAP 4500) with Waters Acuity UPLC BEHC18 chromatographic column (1.7 μm , 50 mm \times 2.1 mm) by BGI (Shenzhen, China).

Chlorophyll measurement

The chlorophyll contents were determined according to previous method with modification (Mao et al., 2011). Briefly, 0.1 g fresh rice leaves were harvested at three leaves stage, squashed with liquid nitrogen, placed into 1 mL chlorophyll extraction solution (1 mM KOH and 80% acetone), and centrifuged at 16000 $\times g$ for 5 min. The supernatant was transferred into a new tube and used for measuring absorbance values at 663-nm and 645-nm wavelengths using a spectrophotometer (DU730, Beckman Coulter, USA), with chlorophyll extraction solution as control.

Contents of Chla and Chlb were calculated by following formula:

$$\text{Chla} = (12.7 \times \text{OD}_{663} - 2.69 \times \text{OD}_{645}) \times V/1000 \times W$$

$$\text{Chlb} = (22.9 \times \text{OD}_{645} - 4.68 \times \text{OD}_{663}) \times V/1000 \times W$$

Where Chla and Chlb represent the contents of Chlorophyll a and Chlorophyll b in leaves (mg/g), V is the volume of the chlorophyll extraction solution (mL), and W is the fresh weight of leaves (g). The chlorophyll contents were the sum of Chla and Chlb, measured by at least three biological replicates.

Lanthanum chloride treatment

The treatment of calcium channel blocker lanthanum chloride (LaCl_3) on rice seedlings was performed as described previously (Shi et al., 2012). Rice seedlings were grown in Yoshida's nutrient solution (Yoshida et al., 1976) under 10 h/14 h light (34827 lux) /dark, light 28–30°C / dark 25°C conditions until three-leaf stage. Then, the seedlings were transferred into another chamber with Yoshida's nutrient solution containing 5 mM LaCl_3 to treat for 4 hours at the same growth conditions. Similarly, the seedlings which grow in Yoshida's nutrient solution without LaCl_3 were as control. Following, the seedlings were transferred into artificial incubator under 10 h /14 h light/dark, at 4°C for 10 hours, and whole plants were harvest for qRT-PCR analysis.

QUANTIFICATION AND STATISTICAL ANALYSIS

Data in figures was expressed as mean \pm SD. RNA-seq experiments was performed in one replicate with qRT-PCR validation and metabolomic profiling were performed for four biological replicates at least. Other replicates in different experiments were stated in

corresponding Figure legends. Significantly enriched biological pathways or metabolic super pathways are performed by hypergeometric test. Correlation analysis is performed by Pearson's correlation. Significantly survival rate, gene expression, or metabolic level difference between different groups were evaluated by Student's t test. $p < 0.05$ were considered as statistical significantly. Significances are represented in the Figures as follows: *, $p < 0.05$; **, $p < 0.01$; ***, $p < 0.001$, unless individual P values as stated.